# imzML Writer: An Easy-to-Use Python Pipeline for Conversion of Continuously Acquired Raw Mass Spectrometry Imaging Files to imzML Format

Joseph Monaghan,[1] Kiera Nguyen,[1] Nicholas Woytowich,[1,2] Alora Keyowski,[1,2] Kyle Duncan[1,2*]

1. Department of Chemistry, Vancouver Island University, 900 Fifth Street, Nanaimo, British Columbia, Canada, V9R 5S5
2. Department of Chemistry, University of Victoria, PO Box 3055, 3800 Finnerty Road, Victoria, British Columbia, Canada, V8P 5C2

* Corresponding author:

Kyle Duncan, Kyle.Duncan@viu.ca

**Abstract:**

Mass spectrometry imaging (MSI) is a powerful tool which reveals the contextual distribution of biomolecules in tissues. Acquiring these images involves collecting an information-rich mass spectrum for each pixel of the ion image, which results in large datasets typically exceeding 1 GB. To streamline data processing and interpretation, various toolboxes have been developed for image pre-processing, segmentation, statistical analysis, and visualization. These generally require imaging data to be input in 'imzML' format, an Extensible Markup Language file with controlled vocabulary for mass spectrometry and MSI-specific parameters. While major/commercial MSI modalities (*e.g.* MALDI) come with proprietary file converters, to our knowledge, no open-access user-friendly converters exist for continuously acquired MSI data (*e.g.* nano-DESI, DESI). Here, we present imzML Writer, an open-access python application which is easy to install and easy to use. imzML Writer has a simple graphical user interface to convert data from MS vendor format into pixel-aligned imzML files suitable for further analysis. We package this application with imzML Scout, a tool to quickly visualize the resulting file(s) and batch export ion images across a range of image/data formats (PNG, TIF, CSV). To demonstrate the utility of files generated by imzML Writer, we processed a nano-DESI image using previously inaccessible toolboxes/data repositories such as Cardinal MSI and METASPACE. Overall, this work provides a simple tool for emerging MSI modality users to access the wealth of advanced MSI processing tools reliant on imzML format.

**Introduction:**

Mass spectrometry imaging (MSI) is emerging as a powerful tool to study the contextual distribution of metabolites, proteins, and drugs in biological tissues.[1] In MSI, information-dense spatial 'omics' data is generated in a two dimensional grid, where pixels simultaneously report the identity and abundance of hundreds to thousands of biomolecules.[2,3] MSI has been applied across many disciplines to help answer both fundamental and applied questions, including the dynamics of host-microbe interactions,[4] drug distribution,[5] mycotoxin localization in food,[6] and intraoperative discrimination of healthy/cancerous tissue.[7,8] There are several MSI techniques available that harness different ionization and sampling approaches to generate spatially resolved mass spectra. Each modality has embedded strengths and limitations.[9] Consequently, there has been an ongoing drive towards multimodal imaging workflows that allow co-registration of multi-omic data, including the spatial metabolome and proteome.[10]

Matrix assisted laser-desorption/ionization (MALDI) is the most widely used MSI modality.[11,12] By rastering laser pulses over the target area, an image grid is constructed with pixel dimensions defined by the focal point of the laser. Several commercial MALDI MSI platforms are available that use vendor specific software to convert the spatially resolved mass spectra into ion images. This data can also be converted to the vendor neutral imzML format, an Extensible Markup Language (XML) format with controlled vocabulary for mass spectrometry and imaging.[13] In the imzML file format, large, GB-sized images are stored in two files: 1) the '.imzML' containing metadata including pixel dimensions, MS model, MS parameters, and scan pattern; and 2) an '.ibd' file containing the MS spectral data in binary format. Powerful open access MSI toolboxes have been developed that read in imzML files, allowing for image segmentation, visualization and co-registration of multimodal images,[14] deep learning for per-pixel classification,[15] and advanced smoothing and segmentation workflows.[16]

The imzML format has been used to a lesser extent in ambient MSI modalities, largely due to how the data is acquired. For example, desorption electrospray ionization (DESI) and nanospray desorption electrospray ionization (nano-DESI) generate MSI data by continuously rastering over tissue surfaces.[3,17–23] As a result, pixel dimensions are defined by the step size between strip lines (y-direction) and the MS scan rate (x-direction). Further, mass analysers involving ion trapping (*e.g.* Orbitrap) use automatic gain control (AGC), which creates dynamic pixel widths and variable numbers of MS scans across each line – features not compatible with the imzML format. It is possible to experimentally fix the AGC target time,[24] but this can compromise the quality of the data, as AGC is needed to provide optimum mass resolution and sensitivity by minimizing space-charge effects.[25] While several custom software tools have been developed by the ambient MSI community to generate publication quality ion images by aligning pixels based on scan time, including ion2image (i2i),[26] msiGen,[27] and MSIQuickview,[28] these platforms do not currently output imzML files. The lack of open access tools to convert ambient MSI data to imzML files restricts ambient MSI users from harnessing many of the open access image processing toolboxes and MSI data repositories that rely on the imzML format (*e.g.* Cardinal MSI,[16] MSIQuant,[29] MSIReader[30], and METASPACE[31]). To our knowledge, there is no open-source, user-friendly program available to convert raw ambient MSI data into the pixel-aligned imzML format.

Here, we present imzML Writer, a cross-platform (Mac, PC) open-access python program to convert continuously acquired ambient MSI data into standardized imzML format via a user-friendly GUI. This software starts with raw vendor format data or mzML files and aligns pixels based on scan time, then writes the aligned MSI data to an imzML file. The software can handle multiple scan filters (including stacked MS/MS experiments) and writes each unique scan filter to a separate imzML and ibd file. Alongside imzML Writer, the toolbox includes imzML Scout, a simple imzML file explorer to inspect, visualize, normalize, and batch export publication quality ion images via a graphical user interface. Overall, imzML Writer allows ambient MSI users access to many of the powerful tools developed for interrogating MSI data that rely on imzML format.

**Materials & Methods:**

*Programming and Testing*

All software development was performed on a personal laptop (Apple Macbook Pro 2023, 8 GB RAM, M3 Chip). Programs were developed in Python 3.12.4 using open-source libraries (numpy, matplotlib, tkinter, pymzML,[32] pyimzML, beautifulsoup4, docker). Additional testing for cross-platform compatibility was performed on a PC workstation (64-bit, 28-core Intel-i7, 32 GB RAM, Windows 11 Pro). All code for imzML Writer and imzML Scout is publicly available on Github https://github.com/VIU-Metabolomics/imzML_Writer.

imzML Writer/Scout have been tested with different vendor formats, instrument types, and interlaced scan functions (Fullscan + MS/MS + tSIM, etc.). Thermo '.raw' datafiles have been most thoroughly vetted, with successful image generation from multiple systems including Orbitrap (Exploris 120, Velos, Q-Exactive; Thermo Scientific, San Jose, CA, USA), FT-ICR (LTQ FT Ultra), and targeted SRM images from a triple quadrupole MS (Fortis). No imaging data was available to us from Waters or Agilent systems. However, pseudo-images were generated from a series of LC-MS and GC-MS runs collected on a Waters Acquity TQD (Missassauga, ON, Canada) and Agilent 7010 system (Agilent Technologies, Santa Clara, CA, USA), respectively.

*Samples & Standards*

LC-MS Optima grade solvents were purchased from Fisher scientific (Mississauga, ON, Canada) including methanol, acetonitrile, water, and formic acid. Example images are generated from purchased rat brain tissue (Sprague-Dawley; Charles River Labs, Winchester, VA, USA). To prepare samples for nano-DESI imaging, tissues were sliced into 12 µm sections using a cryotome (Leica CM 1850 cryomicrotome, Wetzlar, Germany) and thaw-mounted onto regular glass microscope slides (SuperFrost, Fisher Scientific). After sectioning, tissues were stored at -80 °C until imaging.

*nano-DESI imaging*

nanoDESI images were collected on a custom-fabricated source.[33,34] For the nanoDESI capillaries, polyimide-coated fused-silica capillaries were used (ID: 50 µm; OD: 150 µm; Molex, Lisle, IL, USA). The primary and secondary capillaries were first aligned using micromanipulators to provide stable flow and minimal droplet size at 0.5 µL/min delivered via syringe pump (KD LEGATO 180, kd Scientific, Holliston, MA, USA) and 500 µL syringe (Hamilton 1750 Series). To collect images, these capillaries were held fixed and a Zaber XYZ stage (Vancouver, BC, Canada) was used to move the tissue below the capillaries. The stage was controlled using custom LabView software described

previously.[28] Images were collected as horizontal line scans at a scan speed between 40 - 60 µm/sec with a 150 µm step between lines. The carrier/spray solvent consisted of 9:1 MeOH:Water spiked with 0.1% formic acid. Data was collected on an Orbitrap Exploris 120 (Thermo Scientific, San Jose, CA) operated in positive ion mode (spray voltage: +3400 V applied to syringe needle, ion transfer tube temperature: 250 °C, RF lens: 70%). Fullscan data was collected in profile mode at 120 000 resolution (*m/z* 200), resulting in scan frequencies of 4 – 22 Hz. Additional selected ion monitoring experiments or product ion scans were also included, as indicated. Depending on MS resolution/scan rate and the number of distinct scan functions, pixel sizes were between 2.2 – 120 µm along the x-dimension and 150 µm along the y-dimension.

**Results & Discussion**:

imzML Writer and imzML Scout are simple, easy-to-install and easy-to-use packages to write and explore standardized imzML files from ambient mass spectrometry imaging techniques. We focus on techniques that collect continuous data along line scans such as nano-DESI and DESI.[3,17–23] The pipeline is designed to take raw MSI data in proprietary vendor formats and convert them to standardized imzML files by aligning pixels based on scan speed and time (Figure 1).The application builds on several excellent open-source software packages from the MS community, including pymzml,[32] pyimzml, and MSConvert.[35] imzML Writer was written in Python with cross-platform operation in mind, allowing users to directly convert raw instrument files from several major vendors including Thermofisher Scientific, Waters, and Agilent, on both Mac and PC. The user-interface is a simple GUI written in TKinter, requiring minimal programming knowledge to install or operate.

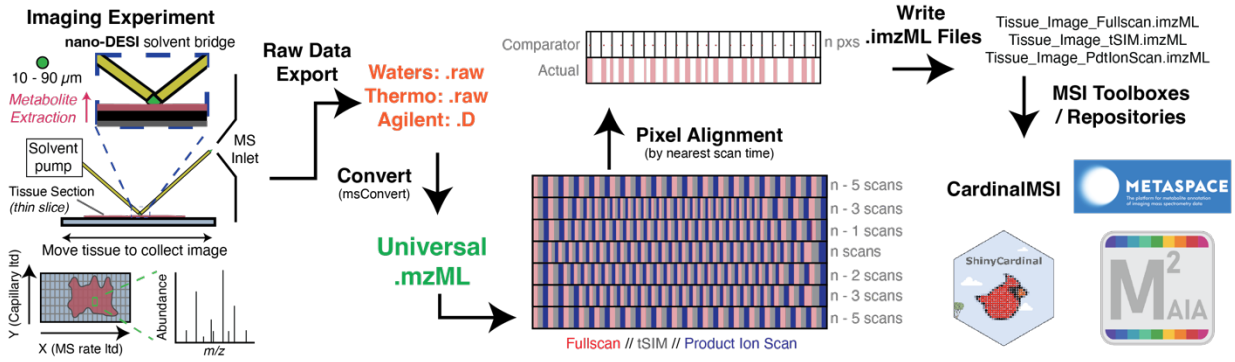


***Figure 1.*** *Workflow for conversion of nanoDESI-MSI data into standard imzML format. Raw imaging data in vendor format is converted to mzML files using MSConvert, the pixel grid is then aligned based on scan time, duplicating pixels in sparsely sampled areas as needed. The resulting imzML file is then annotated with additional metadata provided by the user or extracted from the mzML, which is compatible with standard toolboxes and data repositories.*

To convert an image using the imzML Writer, users navigate to a folder containing data in either raw vendor format or vendor-neutral mzML format (Figure 2A). By clicking 'Full Conversion' or 'mzML to imzML' respectively, the program will begin writing imzML image files (one for each scan type). Optionally, users can include a lock mass for coarse *m/z* recalibration in the resulting imzML file. Progress for each step is reported in the GUI. After writing the imzML file, metadata is populated from the user-input fields (*i.e.*, pixel dimensions) and the source mzML file (MS model/configuration, scan filter).

In the resulting imzML file, ion images can be visualized by selecting a file and clicking the 'view imzML' button. This launches a separate GUI, imzML Scout, to explore the data and batch export ion images (Figure 2B). By clicking a pixel, the corresponding mass spectrum is shown on the right of the screen. Clicking on a *m/z* peak refreshes the ion image to show that *m/z*.

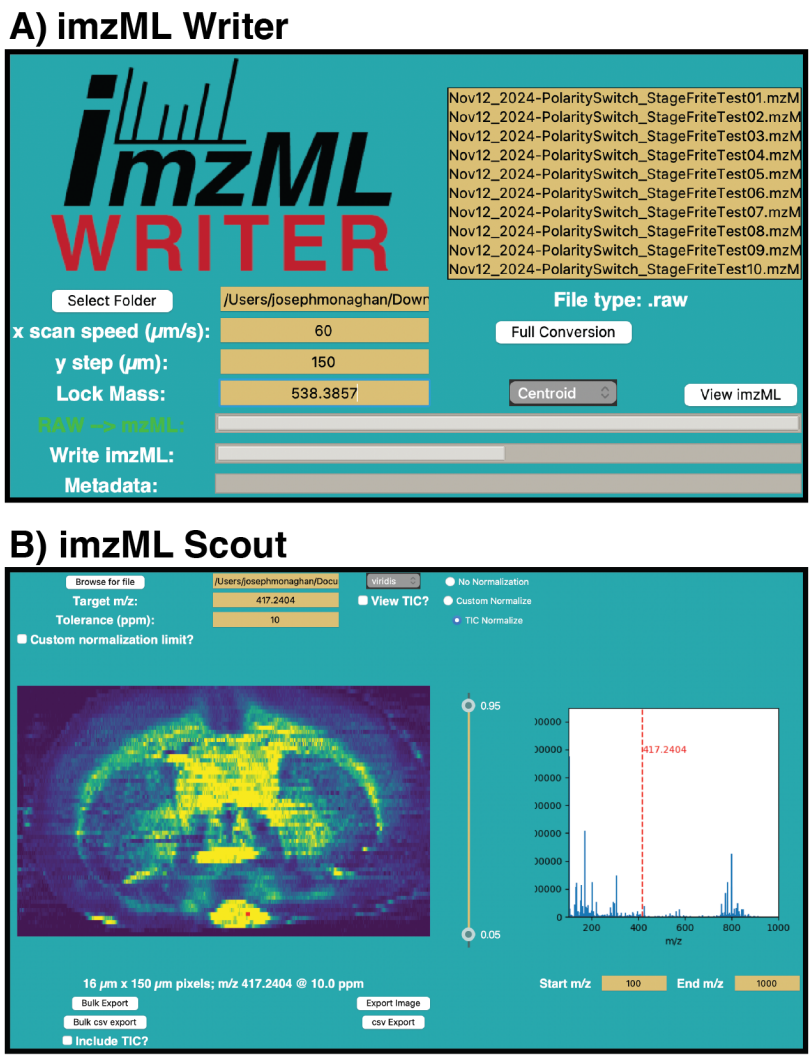


***Figure 2.*** *GUI for imzML Writer (A) and Scout (B). imzML Writer takes line-scan data from vendor-file (.raw, .D) or mzML format and writes image data into an aligned pixel grid in imzML format. Preliminary exploration and export of raw image data (.csv) or high-quality ion images (.tif) can then be performed from the accompanying imzML Scout accessible from the 'view imzML' button or command line.*

### *Data conversion from vendor-file format to imzML*

Before pixel alignment, data is converted from the vendor file format to mzML using MSConvert (Proteowizard).[35] On PC, MSConvert can be installed natively and is called by imzML Writer directly. However, MSConvert is not supported on Mac/Linux and is instead accessed through a docker container. After initial setup (detailed instructions in the README on GitHub), the docker image is called directly and does not need to be manipulated by the user. To ensure compatibility with downstream processing, several keyword arguments are passed to MSConvert, such as 'no compression' and 'SIM/SRM as spectra.' Typically, the data is centroided at this stage for improved processing speed and reduced file sizes. However, both MSConvert and downstream processing in imzML Writer can accommodate profile-mode data. Processing profile data is more

computationally taxing, as demonstrated by the same 862MB raw imaging dataset taking imzML Writer 87.3 s to process in centroid mode (final imzML size: 259.2 MB) and 180.8 s to process in profile mode (final imzML size: 2.37 GB).

To convert from mzML to imzML, a consistent pixel grid is generated for each scan filter. The number of pixels in the Y-direction is defined by the number of line scans collected. However, in the X-direction, variations in ion accumulation time to meet the AGC target can lead to differing numbers of scans across a line and dynamic pixel width.[25,26] To resolve this, each mzML line scan is surveyed to identify the maximum number of pixels needed in the X-direction. The overall time for a line-scan is then split into *max x* target scan times for each pixel. Pixels are then assigned a mass spectrum across each line scan based on the closest (in time) spectrum to that target time (Figure 1). This approach results in some duplicated spectra in adjacent pixels for sparsely sampled regions of the image, providing pseudo-dynamic pixel widths (quantized to pixel dimensions). Overlays of the optical image and ion images generated show no signs of distortion (Figure S1). As spectra are written to the growing imzML file, an optional *m/z* recalibration is performed wherein the lock mass is identified as the highest intensity *m/z* within ±20 ppm of the specified lock mass. Once identified, the ppm offset is calculated, and the entire spectrum is shifted to correct for this offset. In spectra where the lock mass can't be identified, the shift of the last spectrum where the lock mass was found is applied.

One imzML and one ibd file are created for each included scan filter, containing all the mass spectral data but no corresponding metadata. To populate these fields, metadata is retrieved from both the mzML source files (instrument model, scan filter, etc.) and user-input fields in the GUI for imaging-specific details (scan speed, spacing between y lines). These details can then be retrieved by imzML processing tools to calculate the aspect ratio of ion images, allowing them to be automatically presented with physically meaningful dimensions which overlay with optical images (Figure S1).

Because imzML Writer goes through an intermediate step of standard mzML files, it is expected to be vendor-agnostic. We have thoroughly evaluated the pipeline with Thermo '.raw' files, generating ion images for Orbitrap Exploris, Q-Exactive, and Velos models across multiple and stacked scan filters. The pipeline can also be used to process data acquired on with triple quadrupole MS (TSQ Fortis; Figure S2). Raw imaging data for Agilent '.D' and Waters '.raw' images were unavailable to us, but the imzML writer generated pseudo images from GC-MS and LC-MS runs collected on an Agilent 7010 and Waters Acquity TQD, respectively (Figure S3). Note that for Waters data, MSConvert can ignore the '-simAsSpectra' and '-srmAsSpectra' flags, which results in mzML files organized by chromatogram, rather than by spectra. This format cannot be processed by imzML Writer.

The speed of imzML Writer was tested with a series of images ranging from 0.18 – 12.6 GB (Table S1). Overall processing time for the images took 12 s (0.18 GB image), 70 s (1.23 GB), 96 s (1.54 GB), 135 s (3.93 GB), 160 s (5.41 GB), and 970 s (12.6 GB), with an average of 54.6 ± 18.8 s per GB of data. Of the processing time, an average of 51% was spent on writing the mzML files, with 25% and 23% spent on writing and annotating the resulting imzML files, respectively. While reasonable for most image processing workflows, further optimization of the pipeline presented including

parallelization and faster libraries for writing metadata to imzML files will be applied in future versions for larger-scale projects and/or high-resolution images.

### *imzML Scout*

imzML writer was paired with a simple GUI viewing tool, imzML Scout, to explore the data and export high-quality ion images (Figure 2B). This allows users to quickly assess the quality of the generated imzML files. In imzML Scout, users select their target ion and tolerance window using the input fields. Alternatively, by clicking on a pixel in the ion image, the mass spectrum for that pixel is called and users can select a *m/z* peak by clicking on it to update the ion image. Simple normalization to total ion count or custom *m/z* can be performed, as well as contrast adjustment using the sliders.

imzML Scout also provides a batch export tool for both images and raw data as a CSV file. By clicking batch export, users are prompted to select a spreadsheet containing their target analyte list with columns for analyte name and *m/z*. imzML Scout then generates and saves ion images for each target in a new 'images' folder where the imzML file is stored. These images can be written under common file formats (.jpg, .png, .tif) and configured for standard colormaps (*e.g.,* Viridis, Hot, Jet) and custom normalization limits. The batch export feature retains settings from the current viewing window, including file format, normalization settings, and intensity limits. Similarly, the underlying data for these images can be written as CSV files, which are readily imported into Matlab or Python for custom data manipulation or visualization such as cross-scan filter normalization. The intention for imzML Scout is to enable users to quickly assess the integrity of generated imzML files, and to cover the basic functionality needed for targeted MSI workflows. For more advanced processing (segmentation, co-registration), a number of existing tools are available (*e.g.* Cardinal, M2aia).[16,36]

### *Downstream data processing of ambient MSI imzML files*

While writing ambient MSI data to the common imzML format carries many advantages, such as reduced computational time with pre-aligned pixel grids, a driving motivator for the creation of imzML Writer was to access the wealth of tools written to process imzML files, including toolboxes for image interpretation such as Cardinal or M2aia or data repositories such as METASPACE.[14,16]

Fundamental to open science is open data. METASPACE provides an excellent platform to house and annotate spatial metabolomics data.[37] However, it requires images to be uploaded as imzML files, making it inaccessible to many ambient MSI techniques. By passing data through imzML Writer, data can be shared publicly via METASPACE, and users can benefit from the resources provided by the platform including automated metabolite annotation and multi-ion visualization. An example nano-DESI image from Figure 2 is available on METASPACE at https://metaspace2020.eu/annotations?ds=2024-10-01_19h14m04s (Figure S4). For this image, METASPACE identified 753 metabolites at a false discovery rate (FDR) of 10% from the HMDB endogenous database including both small metabolites such as *m/z* 104.1070 (putative ID: choline), *m/z* 170.0326 (putative ID: creatine), and *m/z* 307.0437 (putative ID: inosine) and larger lipid species at *m/z* 768.5878 (putatively $[C_{42}H_{84}NO_7P+Na]^+$), *m/z* 854.5670 (putatively

$[C_{48}H_{82}NO_8P+Na]^+$), and *m/z* 872.5566 (putatively $[C_{48}H_{84}NO_8P+K]^+$). Overall, providing ambient MSI users a means to upload imzML files to METASPACE facilitates easy data sharing, exploration, and interpretation with non-specialized collaborators, and provides an additional layer of backup for these valuable datasets.

Beyond data sharing/storage, the R package Cardinal provides powerful tools for all stages of processing MSI data, including spectral alignment, feature identification, visualization, statistical analysis, and image segmentation.[16] To demonstrate compatibility, an imzML file generated from imzML Writer was loaded into Cardinal to align and segment the example rat brain image using the spatial shrunken centroids tool in a two-stage process.[38] First, the whole image was pre-processed including normalization (root mean square method), peak alignment (10 ppm tolerance), and feature filtration (>10% frequency), resulting in 1408 identified features. An initial segmentation was performed using the whole image to identify tissue and glass slide background (Figure S5), which was used as a mask to crop the image to include only tissue-associated pixels. This cropped image was then further split into 3 – 9 segments (Figure S6), with 7 segments providing the best map to expected anatomical features from the optical image (Figure 3). For example, the corpus callosum (purple) and caudate putamen (green) are readily apparent. The primary and secondary somatosensory regions are visible in the blue and yellow groupings, respectively. The basal forebrain and several central substructures are grouped in red. The remaining groups (dark blue and orange) appear to be artifacts from the nano-DESI experiment. Overall, converting nano-DESI MSI data with imzML Writer provided a simple way to utilize the Cardinal data processing workflows and enabled successful image segmentation based on tissue morphology.

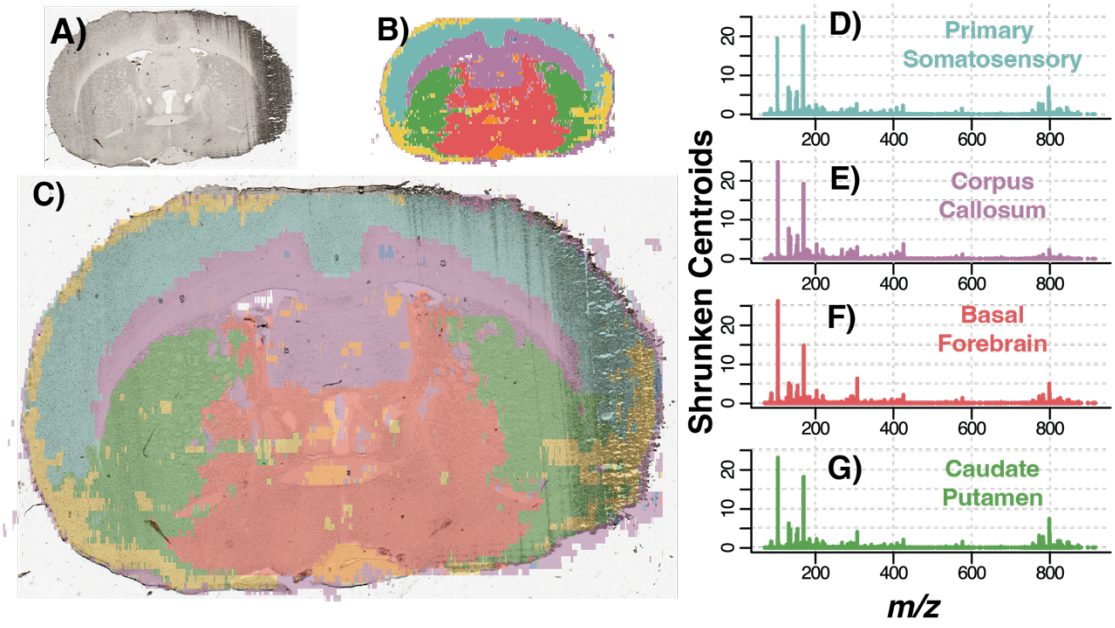


***Figure 3.*** *Spatial Shrunken Centroid Segmentation using Cardinal on a nano-DESI rat brain image. A) Optical Image before nano-DESI analysis. B) Segmented image (r = 1, k = 7, s=0) showing distinct brain regions. C) Overlay of A & B illustrating mapping of anatomical features to distinct regions of the brain. D-G) Shrunken centroids for each segment.*

**Conclusion:**

An open-source program was developed to convert continuously acquired ambient MSI data into standard imzML files. A cross-platform, simple GUI interface converts raw MSI data into pixel-aligned imzML files suitable for use with existing open-source toolboxes and data repositories. The GUI provides a simple control interface to the user, allowing input of imaging-specific details (spacing between strip lines, scan speed), *m/z* recalibration based on a lock mass, and progress updates on the conversion. The resulting imzML file is annotated with these details and additional metadata retrieved from the source file (*e.g.* scan type, MS model). This pipeline can process data across various vendor formats (.raw, .D) and data types (*e.g.* multiple scan filters), and runs on both Mac and PC. The co-packaged imzML Scout provides basic visualization needs, allowing users to specify/select a *m/z* to visualize, or view the individual mass spectrum of a particular pixel. Batch export of images/datasets is possible from a user-specified spreadsheet of metabolites and *m/z*. Generated imzML files are compatible with existing MSI toolboxes and data repositories, including Cardinal and METASPACE – allowing these robust toolboxes and data sharing platforms to be readily accessed by emerging MSI modalities.

**Acknowledgments:**

The authors acknowledge Vancouver Island University and the University of Victoria for ongoing support of graduate students. This work was funded by NSERC (RG-PIN-2022-03696), the Terry Fox Research Institute in combination with the Lotte and John Hecht Memorial Foundation (Program Project Grant #1125), and MITACS Accelerate (IT39215). Key infrastructure was funded through the Canadian Foundation for Innovation (CFI JELF 43810). The authors also greatly acknowledge Drs. Erik Krogh and Chris Gill of the Applied Environmental Research Laboratories (AERL) for access to MS instrumentation (CFI 40274). Salary support for JM was provided through a Michael Smith Health Research BC trainee Fellowship (RT-2024-03771).

**References:**


(1) Ma, S.; Leng, Y.; Li, X.; Meng, Y.; Yin, Z.; Hang, W. High Spatial Resolution Mass Spectrometry Imaging for Spatial Metabolomics: Advances, Challenges, and Future Perspectives. *TrAC Trends Anal. Chem.* **2023**, *159*, 116902. https://doi.org/10.1016/j.trac.2022.116902.

(2) Duncan, K. D.; Pětrošová, H.; Lum, J. J.; Goodlett, D. R. Mass Spectrometry Imaging Methods for Visualizing Tumor Heterogeneity. *Curr. Opin. Biotechnol.* **2024**, *86*, 103068. https://doi.org/10.1016/j.copbio.2024.103068.

(3) Iqfath, M.; Wali, S. N.; Amer, S.; Hernly, E.; Laskin, J. Nanospray Desorption Electrospray Ionization Mass Spectrometry Imaging (Nano-DESI MSI): A Tutorial Review. *ACS Meas. Sci. Au* **2024**, acsmeasuresciau.4c00028. https://doi.org/10.1021/acsmeasuresciau.4c00028.

(4) Sharon, G.; Garg, N.; Debelius, J.; Knight, R.; Dorrestein, P. C.; Mazmanian, S. K. Specialized Metabolites from the Microbiome in Health and Disease. *Cell Metab.* **2014**, *20* (5), 719–730. https://doi.org/10.1016/j.cmet.2014.10.016.

(5) Dannhorn, A.; Swales, J. G.; Hamm, G.; Strittmatter, N.; Kudo, H.; Maglennon, G.; Goodwin, R. J. A.; Takats, Z. Evaluation of Formalin-Fixed and FFPE Tissues for Spatially Resolved Metabolomics and Drug Distribution Studies. *Pharmaceuticals* **2022**, *15* (11), 1307. https://doi.org/10.3390/ph15111307.

(6) Da Silva Lima, G.; Franco Dos Santos, G.; Ramalho, R. R. F.; De Aguiar, D. V. A.; Roque, J. V.; Maciel, L. I. L.; Simas, R. C.; Pereira, I.; Vaz, B. G. Laser Ablation Electrospray Ionization Mass Spectrometry Imaging as a New Tool for Accessing Patulin Diffusion in Mold-Infected Fruits. *Food Chem.* **2022**, *373*, 131490. https://doi.org/10.1016/j.foodchem.2021.131490.

(7) Santilli, A. M. L.; Ren, K.; Oleschuk, R.; Kaufmann, M.; Rudan, J.; Fichtinger, G.; Mousavi, P. Application of Intraoperative Mass Spectrometry and Data Analytics for Oncological Margin Detection, A Review. *IEEE Trans. Biomed. Eng.* **2022**, *69* (7), 2220–2232. https://doi.org/10.1109/TBME.2021.3139992.

(8) Woolman, M.; Katz, L.; Gopinath, G.; Kiyota, T.; Kuzan-Fischer, C. M.; Ferry, I.; Zaidi, M.; Peters, K.; Aman, A.; McKee, T.; Fu, F.; Amara-Belgadi, S.; Daniels, C.; Wouters, B. G.; Rutka, J. T.; Ginsberg, H. J.; McIntosh, C.; Zarrine-Afsar, A. Mass Spectrometry Imaging Reveals a Gradient of Cancer-like Metabolic States in the Vicinity of Cancer Not Seen in Morphometric Margins from Microscopy. *Anal. Chem.* **2021**, *93* (10), 4408–4416. https://doi.org/10.1021/acs.analchem.0c04129.

(9) Alexandrov, T. Spatial Metabolomics and Imaging Mass Spectrometry in the Age of Artificial Intelligence. *Annu. Rev. Biomed. Data Sci.* **2020**, *3* (1), 61–87. https://doi.org/10.1146/annurev-biodatasci-011420-031537.

(10) Neumann, E. K.; Djambazova, K. V.; Caprioli, R. M.; Spraggins, J. M. Multimodal Imaging Mass Spectrometry: Next Generation Molecular Mapping in Biology and Medicine. *J. Am. Soc. Mass Spectrom.* **2020**, *31* (12), 2401–2415. https://doi.org/10.1021/jasms.0c00232.

(11) Buchberger, A. R.; DeLaney, K.; Johnson, J.; Li, L. Mass Spectrometry Imaging: A Review of Emerging Advancements and Future Insights. *Anal. Chem.* **2018**, *90* (1), 240–265. https://doi.org/10.1021/acs.analchem.7b04733.

(12) Lee, P. Y.; Yeoh, Y.; Omar, N.; Pung, Y.-F.; Lim, L. C.; Low, T. Y. Molecular Tissue Profiling by MALDI Imaging: Recent Progress and Applications in Cancer Research. *Crit. Rev. Clin. Lab. Sci.* **2021**, *58* (7), 513–529. https://doi.org/10.1080/10408363.2021.1942781.

(13) Schramm, T.; Hester, Z.; Klinkert, I.; Both, J.-P.; Heeren, R. M. A.; Brunelle, A.; Laprévote, O.; Desbenoit, N.; Robbe, M.-F.; Stoeckli, M.; Spengler, B.; Römpp, A. imzML — A Common Data Format for the Flexible Exchange and Processing of Mass Spectrometry Imaging Data. *J. Proteomics* **2012**, *75* (16), 5106–5110. https://doi.org/10.1016/j.jprot.2012.07.026.

(14) Cordes, J.; Enzlein, T.; Marsching, C.; Hinze, M.; Engelhardt, S.; Hopf, C.; Wolf, I. M2aia—Interactive, Fast, and Memory-Efficient Analysis of 2D and 3D Multi-Modal Mass Spectrometry Imaging Data. *GigaScience* **2021**, *10* (7), giab049. https://doi.org/10.1093/gigascience/giab049.
(15) Cordes, J.; Enzlein, T.; Hopf, C.; Wolf, I. pyM2aia: Python Interface for Mass Spectrometry Imaging with Focus on Deep Learning. *Bioinformatics* **2024**, *40* (3), btae133. https://doi.org/10.1093/bioinformatics/btae133.
(16) Bemis, K. A.; Föll, M. C.; Guo, D.; Lakkimsetty, S. S.; Vitek, O. Cardinal v.3: A Versatile Open-Source Software for Mass Spectrometry Imaging Analysis. *Nat. Methods* **2023**, *20* (12), 1883–1886. https://doi.org/10.1038/s41592-023-02070-z.
(17) Smith, M. J.; Nie, M.; Adner, M.; Säfholm, J.; Wheelock, C. E. Development of a Desorption Electrospray Ionization–Multiple-Reaction-Monitoring Mass Spectrometry (DESI-MRM) Workflow for Spatially Mapping Oxylipins in Pulmonary Tissue. *Anal. Chem.* **2024**, *96* (45), 17950–17959. https://doi.org/10.1021/acs.analchem.4c02350.
(18) Kumar, B. S. Desorption Electrospray Ionization Mass Spectrometry Imaging (DESI-MSI) in Disease Diagnosis: An Overview. *Anal. Methods* **2023**, *15* (31), 3768–3784. https://doi.org/10.1039/D3AY00867C.
(19) Jiang, L.; Hilger, R. T.; Laskin, J. Hardware and Software Solutions for Implementing Nanospray Desorption Electrospray Ionization (nano-DESI) Sources on Commercial Mass Spectrometers. *J. Mass Spectrom.* **2024**, *59* (7), e5065. https://doi.org/10.1002/jms.5065.
(20) Weigand, M. R.; Moore, A. M.; Hu, H.; Angel, P. M.; Drake, R. R.; Laskin, J. Imaging of N-Linked Glycans in Biological Tissue Sections Using Nanospray Desorption Electrospray Ionization (Nano-DESI) Mass Spectrometry. *J. Am. Soc. Mass Spectrom.* **2023**, *34* (11), 2481–2490. https://doi.org/10.1021/jasms.3c00209.
(21) Marques, C.; Friedrich, F.; Liu, L.; Castoldi, F.; Pietrocola, F.; Lanekoff, I. Global and Spatial Metabolomics of Individual Cells Using a Tapered Pneumatically Assisted Nano-DESI Probe. *J. Am. Soc. Mass Spectrom.* **2023**, *34* (11), 2518–2524. https://doi.org/10.1021/jasms.3c00239.
(22) Mavroudakis, L.; Lanekoff, I. Identification and Imaging of Prostaglandin Isomers Utilizing $MS^3$ Product Ions and Silver Cationization. *J. Am. Soc. Mass Spectrom.* **2023**, *34* (10), 2341–2349. https://doi.org/10.1021/jasms.3c00233.
(23) Abbassi-Ghadi, N.; Antonowicz, S. S.; McKenzie, J. S.; Kumar, S.; Huang, J.; Jones, E. A.; Strittmatter, N.; Petts, G.; Kudo, H.; Court, S.; Hoare, J. M.; Veselkov, K.; Goldin, R.; Takáts, Z.; Hanna, G. B. *De Novo* Lipogenesis Alters the Phospholipidome of Esophageal Adenocarcinoma. *Cancer Res.* **2020**, *80* (13), 2764–2774. https://doi.org/10.1158/0008-5472.CAN-19-4035.
(24) Schneemann, J.; Schäfer, K.-C.; Spengler, B.; Heiles, S. IR-MALDI Mass Spectrometry Imaging with Plasma Post-Ionization of Nonpolar Metabolites. *Anal. Chem.* **2022**, *94* (46), 16086–16094. https://doi.org/10.1021/acs.analchem.2c03247.
(25) Eliuk, S.; Makarov, A. Evolution of Orbitrap Mass Spectrometry Instrumentation. *Annu. Rev. Anal. Chem.* **2015**, *8* (1), 61–80. https://doi.org/10.1146/annurev-anchem-071114-040325.
(26) Lillja, J.; Duncan, K. D.; Lanekoff, I. Ion-to-Image, I2i, a Mass Spectrometry Imaging Data Analysis Platform for Continuous Ionization Techniques. *Anal. Chem.* **2023**, *95* (31), 11589–11595. https://doi.org/10.1021/acs.analchem.3c01615.
(27) Hernly, E.; Hu, H.; Laskin, J. MSIGen: An Open-Source Python Package for Processing and Visualizing Mass Spectrometry Imaging Data. *J. Am. Soc. Mass Spectrom.* **2024**, *35* (10), 2315–2323. https://doi.org/10.1021/jasms.4c00178.
(28) Lanekoff, I.; Heath, B. S.; Liyu, A.; Thomas, M.; Carson, J. P.; Laskin, J. Automated Platform for High-Resolution Tissue Imaging Using Nanospray Desorption Electrospray Ionization Mass Spectrometry. *Anal. Chem.* **2012**, *84* (19), 8351–8356. https://doi.org/10.1021/ac301909a.

(29) Källback, P.; Nilsson, A.; Shariatgorji, M.; Andrén, P. E. msIQuant – Quantitation Software for Mass Spectrometry Imaging Enabling Fast Access, Visualization, and Analysis of Large Data Sets. *Anal. Chem.* **2016**, *88* (8), 4346–4353. https://doi.org/10.1021/acs.analchem.5b04603.
(30) Bokhart, M. T.; Nazari, M.; Garrard, K. P.; Muddiman, D. C. MSiReader v1.0: Evolving Open-Source Mass Spectrometry Imaging Software for Targeted and Untargeted Analyses. *J. Am. Soc. Mass Spectrom.* **2018**, *29* (1), 8–16. https://doi.org/10.1007/s13361-017-1809-6.
(31) Palmer, A.; Phapale, P.; Chernyavsky, I.; Lavigne, R.; Fay, D.; Tarasov, A.; Kovalev, V.; Fuchser, J.; Nikolenko, S.; Pineau, C.; Becker, M.; Alexandrov, T. FDR-Controlled Metabolite Annotation for High-Resolution Imaging Mass Spectrometry. *Nat. Methods* **2017**, *14* (1), 57–60. https://doi.org/10.1038/nmeth.4072.
(32) Kösters, M.; Leufken, J.; Schulze, S.; Sugimoto, K.; Klein, J.; Zahedi, R. P.; Hippler, M.; Leidel, S. A.; Fufezan, C. pymzML v2.0: Introducing a Highly Compressed and Seekable Gzip Format. *Bioinformatics* **2018**, *34* (14), 2513–2514. https://doi.org/10.1093/bioinformatics/bty046.
(33) Nguyen, K.; Carleton, G.; Lum, J. J.; Duncan, K. D. Expanding Spatial Metabolomics Coverage with Lithium-Doped Nanospray Desorption Electrospray Ionization Mass Spectrometry Imaging. *Anal. Chem.* **2024**, acs.analchem.4c03553. https://doi.org/10.1021/acs.analchem.4c03553.
(34) Duncan, K. D.; Sun, X.; Baker, E. S.; Dey, S. K.; Lanekoff, I. In Situ Imaging Reveals Disparity between Prostaglandin Localization and Abundance of Prostaglandin Synthases. *Commun. Biol.* **2021**, *4* (1), 966. https://doi.org/10.1038/s42003-021-02488-1.
(35) Chambers, M. C.; Maclean, B.; Burke, R.; Amodei, D.; Ruderman, D. L.; Neumann, S.; Gatto, L.; Fischer, B.; Pratt, B.; Egertson, J.; Hoff, K.; Kessner, D.; Tasman, N.; Shulman, N.; Frewen, B.; Baker, T. A.; Brusniak, M.-Y.; Paulse, C.; Creasy, D.; Flashner, L.; Kani, K.; Moulding, C.; Seymour, S. L.; Nuwaysir, L. M.; Lefebvre, B.; Kuhlmann, F.; Roark, J.; Rainer, P.; Detlev, S.; Hemenway, T.; Huhmer, A.; Langridge, J.; Connolly, B.; Chadick, T.; Holly, K.; Eckels, J.; Deutsch, E. W.; Moritz, R. L.; Katz, J. E.; Agus, D. B.; MacCoss, M.; Tabb, D. L.; Mallick, P. A Cross-Platform Toolkit for Mass Spectrometry and Proteomics. *Nat. Biotechnol.* **2012**, *30* (10), 918–920. https://doi.org/10.1038/nbt.2377.
(36) Dong, Y.; Heinig, U. Mass Spectrometry Imaging Data Analysis with ShinyCardinal. March 12, 2024. https://doi.org/10.21203/rs.3.rs-4072606/v1.
(37) Alexandrov, T.; Ovchinnikova, K.; Palmer, A.; Kovalev, V.; Tarasov, A.; Stuart, L.; Nigmetzianov, R.; Fay, D.; Key METASPACE contributors; Gaudin, M.; Lopez, C. G.; Vetter, M.; Swales, J.; Bokhart, M.; Kompauer, M.; McKenzie, J.; Rappez, L.; Velickovic, D.; Lavigne, R.; Zhang, G.; Thinagaran, D.; Ruhland, E.; Sans, M.; Triana, S.; Sammour, D. A.; Aboulmagd, S.; Bagger, C.; Strittmatter, N.; Rigopoulos, A.; Gemperline, E.; Joensen, A. M.; Geier, B.; Quiason, C.; Weaver, E.; Prasad, M.; Balluff, B.; Nagornov, K.; Li, L.; Linscheid, M.; Hopf, C.; Heintz, D.; Liebeke, M.; Spengler, B.; Boughton, B.; Janfelt, C.; Sharma, K.; Pineau, C.; Anderton, C.; Ellis, S.; Becker, M.; Pánczél, J.; Violante, G. D.; Muddiman, D.; Goodwin, R.; Eberlin, L.; Takats, Z.; Shahidi-Latham, S. METASPACE: A Community-Populated Knowledge Base of Spatial Metabolomes in Health and Disease. February 3, 2019. https://doi.org/10.1101/539478.
(38) Bemis, K. D.; Harry, A.; Eberlin, L. S.; Ferreira, C. R.; Van De Ven, S. M.; Mallick, P.; Stolowitz, M.; Vitek, O. Probabilistic Segmentation of Mass Spectrometry (MS) Images Helps Select Important Ions and Characterize Confidence in the Resulting Segments. *Mol. Cell. Proteomics* **2016**, *15* (5), 1761–1772. https://doi.org/10.1074/mcp.O115.053918.